Three-photon excitation of quantum two-level systems

Viviana Villafañe,[1,*] Bianca Scaparra,[1,*] Manuel Rieger,[1] Stefan Appel,[1] Rahul Trivedi,[2] Rachel Oliver,[3] Robert Taylor,[4] Jonathan J. Finley,[1] and Kai Mueller[1,†]

[1] *Walter Schottky Institut and Physik Department, Technische Universität München, Am Coulombwall 4, 85748 Garching, Germany*
[2] *Max-Planck-Institute for Quantum Optics, Hans-Kopfermann-Str. 1, 85748 Garching, Germany*
[3] *Department of Materials Science, University of Cambridge, Cambridge, United Kingdom of Great Britain and Northern Ireland*
[4] *University Oxford, Dept Phys, Clarendon Lab, Parks Rd, Oxford OX1 3PU, England*

We experimentally demonstrate the long-standing fundamental theoretical prediction that quantum two-level systems can only be efficiently resonantly excited via multi-photon pulses containing an odd number of photons. This prediction can directly be seen from time-dependent Floquet theory that also allows to quantify the strength of the multi-photon processes. For the experimental demonstration, we perform spectroscopy measurements on a single InGaN quantum dot with a variety of laser detunings, and observe that the system can be excited in a resonant three-photon process, while resonant two-photon excitation is entirely suppressed. Finally, we exploit this technique to probe intrinsic properties of InGaN quantum dots. In contrast to non-resonant excitation, slow relaxation of charge carriers is avoided which allows to directly measure the radiative lifetime of the lowest energy exciton states. Since the emission energy is far detuned from the resonant driving laser field polarization filtering is not required and emission with a larger degree of linear polarization is observed compared to non-resonant excitation.

Optically-active few-level quantum systems play a pivotal role for probing fundamentals of light-matter interactions and for realizing building blocks for photonic quantum technologies. In the solid-state, color centers and semiconductor quantum dots are prominent systems for these tasks due to their strong coupling to light. Coherent control of electrons in quantum dots via optically-tailored pulsed lasers is a widely used technique to induce a precise quantum evolution of the electrons under strong-field interaction, which can manifest in strong-field observables such as the Mollow triplet, Ramsey interference, and Rabi oscillations[1–7]. Most of these techniques are well established and demonstrate good agreement between theoretical predictions and experimental measurements. Nonetheless, as long ago as 1965, Shirley et al. [8] predicted a fundamental quantum mechanical result, the confirmation of which has remained elusive until today. In his paper, Shirley proposed that any generic two-level quantum system can only be excited using an *odd* number of photons. Even though this selection rule arises from the simplest Hamiltonian describing a two-level system driven by a strong laser field, it represents a fundamental expectation of quantum mechanics. The experimental confirmation of this selection rule continued to be a challenge for several years due to (i) the need of a pristine two-level system composed of a ground and a excited state without any intermediate real states; (ii) the prerequisite for high peak power intensities of the laser field to perform multi-photon absorption experiments; and (iii) the long wavelengths used in a multi-photon experiment as compared to the emission wavelength of the two-level system.

Semiconductor quantum dots (QDs) formed from group-III nitrides are a promising quantum platform for near future applications. Their large energy bandgap and well developed epitaxial growth methods permit the fabrication of bright QDs having fast radiative decay times and on-demand emission of single photons at elevated temperatures (200K). These properties open the way towards achieving quantum light sources for quantum photonic technologies with significant scope for devices at elevated temperatures. [9–12]. Indium gallium nitride QDs are particularly attractive since their emission energy lies in the blue and green spectral region, a range well-matched to commercially available ultrafast single photon detectors and easily reachable for multi-photon absorption experiments [13, 14].

In this letter, we present an experimental demonstration of Shirley's selection rule by exploring multi-photon excitation of individual InGaN quantum dots. We model our results using the full Floquet Hamiltonian to describe the complete system evolution, the simplest Hamiltonian describing an optically driven two-level system, and obtain good qualitative agreement. Our findings are very general, and are expected to hold true for many different quantum systems. Moreover, our results reveal new information about the optical properties of the InGaN QDs when subject to resonant excitation. The resonant character of the excitation allows to directly measure the radiative lifetime, which under non-resonant excitation is obscured by slow carrier relaxation processes. Intrinsically different from standard resonant excitation of excitons and biexcitons, in our stratagem the QD emission energy is far detuned from the resonant driving laser field and thus no polarization filtering is required. Finally, we observe a higher degree of linear polarization compared

to traditional off-resonant excitation commonly used for group-II nitride quantum dots.

The QDs under study are non-polar (11-20) a-plane InGaN QDs grown by metal-organic vapour phase epitaxy (MOVPE) embedded within a p-i-n doped gallium nitride (GaN) matrix[15]. This a-plane growth minimizes the unwanted quantum-confined Stark effect (QCSE) that is usually present in nitride-based QDs, increasing the quantum efficiency and reducing coupling to vibrational modes that can introduce a significant non-radiative channel[9, 16, 17]. InGaN QDs are positioned in the centre of a 50 nm thick intrinsic GaN layer, which is clad by a 600 nm thick layer of n-doped GaN and a 200 nm thick layer of p-doped GaN, as shown on the inset of Fig.1(a). Nanopillar structures of radius ∼150 nm are fabricated surrounding the QDs to allow for increased photon extraction efficiencies by drop-casting of silica nanospheres onto the wafer as an etch mask, followed by dry etching to a depth of ∼350 nm. The residual silica nanosphere etch mask is then removed by ultrasonication and a buffered-oxide etch.

An ultrafast laser setup is used to study the multi-photon excitation of the InGaN QDs. Hereby, single nanopillars are excited by ∼100 fs tunable laser pulses tunable within the 0.8-1.51 eV range generated by a mode-locked Ti:sapphire laser that seeds an optical parametric oscillator having a repetition frequency of 80MHz. The excitation laser is focused onto the sample through a Cassegrain objective lens (25x, 0.4 N.A.), with emission collected via the same objective. We use a reflective objective to avoid chromatic aberrations between the excitation and detection wavelengths. The excitation laser is separated from the measured PL using a dichroic mirror. Fig.1(a) presents typical microluminescence spectra (μ-PL) taken on two single InGaN QDs embedded in nanopillars at 4K. The spectra possesses two sharp features identified as single QDs in the green-blue spectral region and is obtained using an excitation energy of 800 nm (1.55 eV) corresponding to a two-photon absorption (PL-2PA) into the continuum bands arising from side quantum wells (SQWs) in the InGaN structure [18, 19]. The single lines have characteristic asymmetric lineshapes, indicative of zero phonon transitions from individual InGaN QDs with coupling to a continuum of acoustic phonons. The QD emission appears on top of a low intensity background caused by fragmented remaining InGaN quantum wells in the sample [15].

The quantum level scheme of the experiments performed in this work is depicted schematically in Fig.1(b). It consists of a InGaN QD having a ground and excited orbital states within the GaN gap. As previously stated, typically QD μ-PL is obtained performing a PL-2PA into the continuum states of the SQWs, as depicted on the left panel. The ground and excited state of the QD system can also be resonantly coupled by driving either a two- or three-photon absorption process using a laser pulse (solid orange arrows) tuned to be resonant on virtual levels (VL) inside the QD, depicted in the middle and left panels of Fig.1(b).

Fig.1(c) shows the emission intensity of a single dot as the excitation energy laser is tuned throughout the two-photon resonance with the SQWs continuum in the GaN matrix. When the laser excitation energy E_L is greater than approximately half of the SQWs interband transition energy $E_S/2$, the single QD emission is clearly observed in the spectra at E_{QD} ∼2.61 eV. As E_L is decreased, the QD emission progressively reduces until it vanishes when $E_L = E_{QD}/2$, corresponding to the resonant 2PA into the QD. The striking disappearance of the QD emission is further emphasized by the presence of the second harmonic generation (SHG) of the SQWs that can clearly be observed in Fig.1(b) [20, 21]. Interestingly, the intensity of the single QD emission exhibits a sharp resonance when approaching the resonant three photon condition, depicted in Fig.1(d) and highlighted with a dashed horizontal white line. Note that in this case we observe not only the QD emission but also the presence of a red-shifted defect band at ∼2.25 eV arising from dislocations on the bulk GaN matrix [22, 23]. In contrast, for the case of the Res-2PA excitation we measure the QD signal on top of an underlying background that arises from InGaN quantum wells [15]. As a consequence, the QD spectra obtained with a resonant 3PA presents a clearer and sharper signature and a better signal-to-noise ratio. This result already highlights one striking advantage of our excitation strategy; while resonant excitation usually requires cross-polarized filtering in the optical setup to distinguish between excitation laser and the generated single photons, the non-linear three-photon excitation presented in this letter allows simple spectral filtering using only a dichroic mirror in the experimental setup.

Fig.2 summarizes the main results of our experiments, focusing on the detuning dependence of the amplitude of the InGaN QD PL. We first draw the readers attention to the experimental absorption cross-sections presented in Fig. 2(a) and extracted from the data presented in Fig. 1. Several features can be highlighted: (i) We observe a strong resonant enhancement of the QD signal close to to the 3PA condition. This resonance is energetically-sharp with a linewidth that corresponds to the spectral bandwidth of the excitation pulse (FWHM∼20 meV at 0.88 eV). (ii) The QD PL intensity drops when tuning the laser energy to the Res-2PA energy, and (iii) the QD intensity rises again when performing a two-photon absorption into the continuum states of the SQWs.

It is worthwhile noticing that it is possible to measure a non-zero 2PA in typical semiconductor colloidal quantum dots, such as ZnSe and ZnSe/ZnS core-shell QDs. In these cases, the resonant 2PA absorption selection rule is determined by the superposition of molecular orbitals HOMO and LUMO (rather than discreet

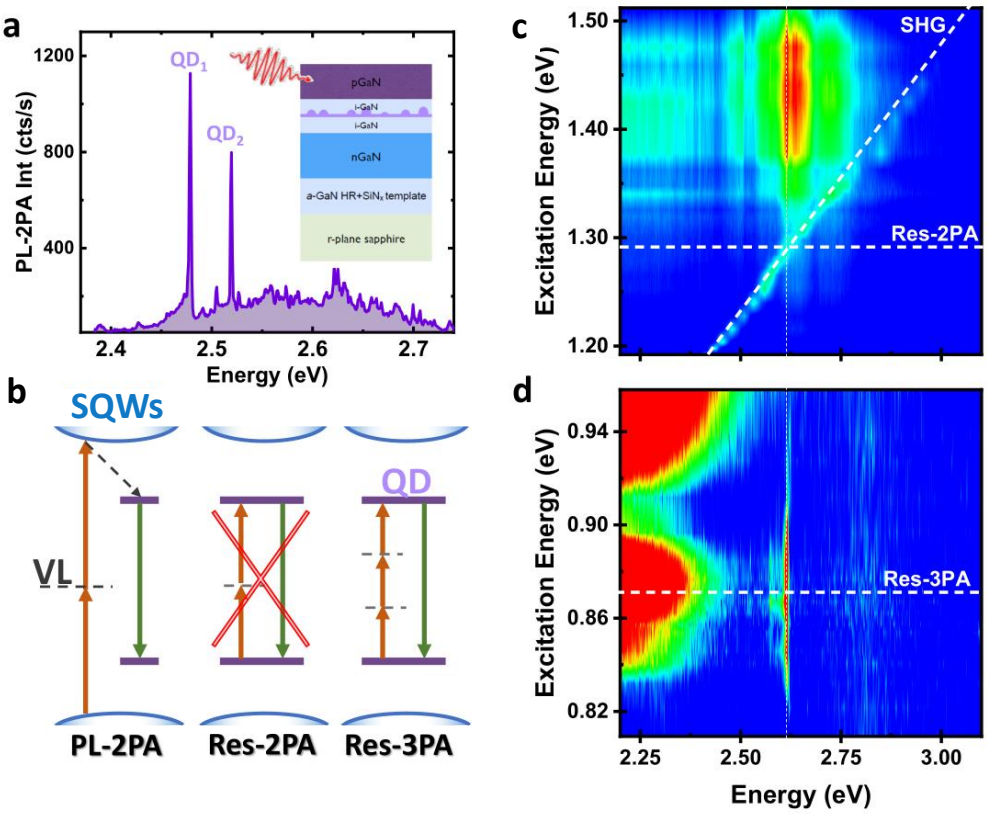

FIG. 1: (a) Photoluminescence spectra acquired using 1.512 eV of excitation energy, corresponding to a 2PA into the GaN continuum. The inset shows a schematic of the sample structure and materials. (b) Scheme of the different experiments presented in this manuscript. Left panel: 2PA into the continuum of the GaN semiconductor. Center panel (Left panel): 2PA (3PA) resonant to the QD levels inside the GaN gap. The resonant 3PA condition is highlighted with a dashed horizontal line. (c) (False Color Image) Measured amplitude of the QD intensity as a function of the laser excitation energy. For clarity, the dashed vertical line highlights the QD emission (∼2.61 eV) and the transverse dashed line the SHG from the GaN. The 2PA resonant condition, at ∼1.3 eV, is also marked by an horizontal line and calls attention to the disappearance of the QD spectra in the vicinity of those energies. (d) (False Color Image) Measured amplitude of the QD intensity as a function of the laser excitation energy for energies close to the 3PA in the QD. The horizontal dashed line highlights the resonant three photon excitation.

single-particle levels), the degree of electronic passivation in the QD surface and the localization of charge carriers in these core-shell quantum heterostructures[24]. Conversely, CdSe colloidal dots present a resonant 2PA signal due to the presence of real intermediate states in between the excitation levels, that enhances the second order absorption coefficient [25]. Both of the aforementioned systems are are not addressed by the Shirley result described in this manuscript, since the selection rule indicates that a single particle in a discreet two-level system without any real intermediate levels can only be excited by an odd number of photons.

An interesting point to be made is that the experimental selection rule observed for InGaN QDs cannot be explained by arguments drawn from classical physics. As previously stated, the QDs presented in this work are grown along one of the non-polar planes of the Wurtzite group-III nitride. Consequently, this non-centrosymmetric system possesses a non-zero second-order susceptibility $\chi^{(2)} \sim 1.3 \times 10^{-11}$ m/V and a third order susceptibility $\chi^{(3)} \sim 5.3 \times 10^{-19}$ m^2/V^2 [20]. Taking into account the power density used in the experiments of Fig.1, if our signal is being generated by SHG and THG processes in the SQWs, the ratio of electric dipole moments for the 2PA and 3PA excitation would be $P^{(2)}/P^{(3)} \sim 350$. This would imply that the QD PL measured with a resonant 2PA excitation is much brighter than the one measured with a resonant 3PA, in strong contrast to our experimental findings.

To theoretically model our system and reproduce the measured quantum optical selection rules we solve the time-dependent Schrödinger equation that describes the interaction of a two-level system with a strong laser field

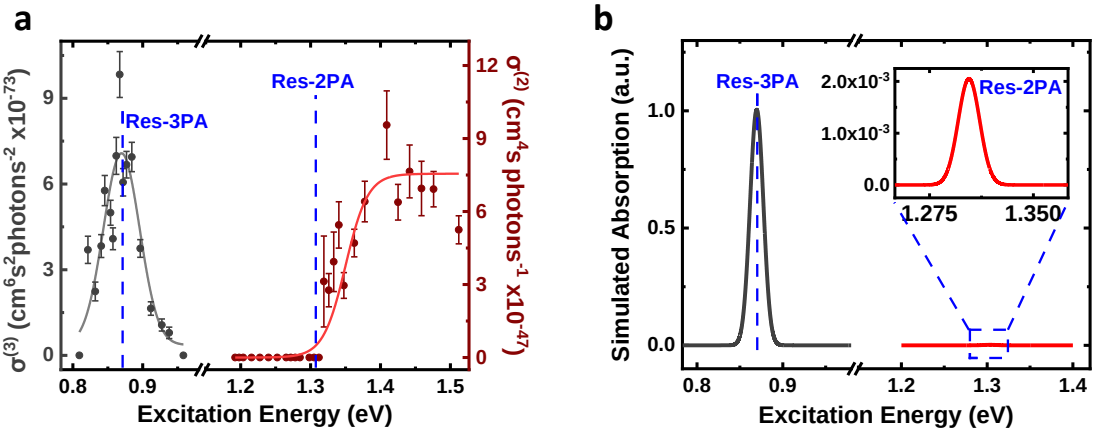

FIG. 2: Experimental (a) and theoretical (b) absorption cross sections of a single InGaN QD as a function of the excitation energy. the resonant 2PA and 3PA conditions are highlighted by the blue vertical dashed lines.

[8]:

$$i\frac{d}{dt}\begin{pmatrix} a_\alpha(t) \\ a_\beta(t) \end{pmatrix} = \hat{\mathcal{H}}(t)\begin{pmatrix} a_\alpha(t) \\ a_\beta(t) \end{pmatrix}, \tag{1}$$

where

$$\hat{\mathcal{H}}(t) = \begin{pmatrix} \omega_0/2 & 2b\sin(\omega t) \\ 2b\sin(\omega t) & -\omega_0/2 \end{pmatrix}. \tag{2}$$

In Eq.1, ω denotes the laser frequency and ω_0 the energy difference between the ground and excited states, denoted as α and β, respectively. b is the mean electric field intensity and $a_{\alpha,\beta}(t)$ are the probability amplitudes of occupation of the ground and excited states in the QD. We calculate the quasienergies q_i, $i = 1, 2$, of the Hamiltonian $\hat{\mathcal{H}}$ for varying energy splittings ω_0 and constant ratios b/ω using the Floquet solver of the python package QuTiP [26, 27].

To estimate the electric field amplitude b, we calculate the transition dipole moment [28] for a typical measured radiative lifetime of 250 ps

$$|M_{21}| = \sqrt{\frac{3\epsilon_0 c^3\hbar}{\tau \cdot 8\pi^2\omega_0^3 n_{\mathrm{GaN}}}} \approx 0.15\, e\,\mathrm{nm}, \tag{3}$$

where $\hbar$ is Planck's constant, ϵ_0 is the vacuum permittivity, c is the speed of light and n_{GaN} is the gallium nitride refraction index. We find that $|M_{21}| \sim 0.15\, e\,\mathrm{nm}$, which is in the same order of magnitude as literature values for similar InGaN/GaN quantum dots [29]. Considering that we use a pulsed laser, we have an average electric field amplitude, E_0, of $\sqrt{2I_{avg}/(c\epsilon_0 \cdot 80\,\mathrm{MHz} \cdot 100\,\mathrm{fs})} = 5.2\,\mathrm{MV/cm}$ during the pulse. The constant b is half the Rabi frequency, which we calculate from the measured power density at three photon absorption ($283\,\mathrm{kW/cm^2}$) as $b = |M_{21}| \cdot E_0/(2\hbar) = 58.8\,\mathrm{THz}$. After establishing the quantitative values of the parameters needed for our calculations, we compute the average transition probabilities $\bar{P}_{\alpha\to\beta}$ from the quasienergies considering that

$$\bar{P}_{\alpha\to\beta} = [1 - 4(\partial q/\partial\omega_0)^2][8]. \tag{4}$$

Panel (b) in Fig. 2 presents the simulated absorption coefficient using Eq. 4. Essentially, the simulation presents two peaks positioned at the Res-2PA and Res-3PA condition. The measured resonance is a convolution of the spectral width of the ultrashort pulses and the simulated absorption peaks (see Fig.2 (b)). The smaller linewidth of Res-2PA decreases the height of the convoluted resonance, making it practically immeasurable. The model predicts an intensity ∼2000 times smaller for the Res-2PA as compared to the Res-3PA condition. The simulation does not describe the rise in intensity resulting from the PL-2PA absorption into the SQWs continuum since it only models a two-level system. Our calculations prove that the measured spectra are mostly determined by the amplitude probability of an electron to be promoted from the ground to the excited state in the QD. It is remarkable that this simple and elegant Hamiltonian which describes many quantum systems is sufficient to describe the selection rule that we observe here experimentally.

To fully understand the nature of the spectra obtained with the Res-3PA condition, where $E_L = E_{QD}/3$, we explore the optical properties of the QD photon emission. Hereby, we isolated the QD emission energy using tunable bandpass filters. Fig. 3 (a) shows the integrated PL intensity of the QD as a function of incident power in logarithmic scale. We observe a cubic characteristic power exponent equal to (2.9±0.3), as expected for a 3PA process. Hereafter, we performed polarization resolved measurements on the PL-2PA and Res-3PA excitation condition and compared the results. Sinusoidal fittings

in accordance with Malus law show that the emission is linearly polarised in agreement with previous work, showing that not only the InGaN QDs present a linearly polarised emission, but also a deterministic polarisation axis along the m-direction of the nitride Wurzite system[9]. Remarkably, the degree of linear polarization DOLP $= (I_{max} - I_{min})/(I_{max} + I_{min})$ is enhanced from 74% for the PL-2PA to 87% when performing a resonant 3PA excitation (Fig. 3(b)).

Finally, we investigate the time-resolved PL-intensity for the filtered QD signal for the PL-2PA and Res-3PA excitation conditions presented in Fig.3(c). We used a single-photon avalanche diode (SPAD) and a time-correlated single photon counting (TCSPC) module triggered by the laser to measure the time traces of the QD PL. The radiative lifetime of the InGaN QD was obtained by fitting the temporal trace with a convolution between a Gaussian function and an exponential decay. The width of the Gaussian function was fitted in accordance with the instrument response function of the SPAD counter. The fitting gives an exponential component with a decay constant of (440 ± 20) ps for PL-2PA experiment, decreasing to (260 ± 20) ps in the 3PA resonant condition. The measured decay times are fast compared to the typical values obtained for c-plane InGaN QDs indicating that the QCSE in this sample is minimized. The observed decrease in the radiative decay time when performing a resonant excitation can be explained as follows: With a PL-2PA excitation we pump carriers into the SQW continuum, that then thermalize and can decay directly into the QD. Therefore, the extracted decay time reflects both the radiative exciton lifetime and slow carrier relaxation processes into the radiative state. In contrast, the Res-3PA case gives direct access to the true radiative lifetime since carrier relaxation does not take place. This indicates that the resonant 3PA excitation scheme can be used to achieve faster repetition rates than the traditional PL-2PA excitation commonly used for InGaN QDs and, moreover, the associated jitter in the single photon emission events is minimized. Overall, the Res-3PA excitation improves the DOLP of the photonic emission and the radiative decay time up to the GHz regime.

In summary, we demonstrated that archetypal two-level systems can only be excited by an odd number of photons, provided that the level structure does not contain real states in between the ground and excited states. To this end, we presented spectroscopy measurements with a wide variety of laser excitation energies in a single InGaN QD and modelled the results using the full Floquet Hamiltonian describing the system evolution. Since the Hamiltonian used in this work is the simplest form describing any optically-driven two-level system, our results prove to hold true for a wide variety of quantum systems. We also showed that our excitation scheme involving the resonant 3PA of InGaN QDs enhances the degree of polarization and and gives direct access time to

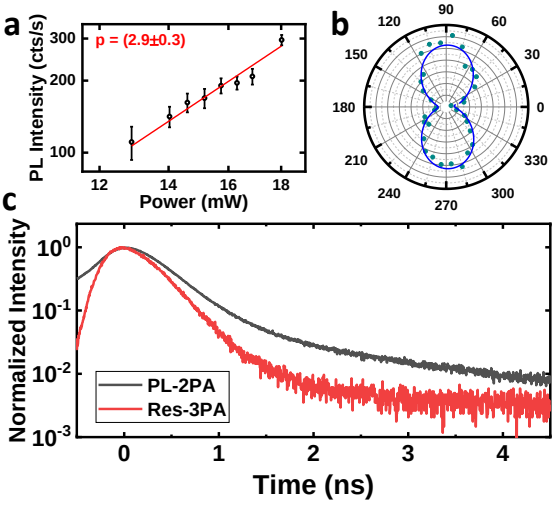

FIG. 3: (a) Power dependence of the InGaN PL when performing a resonant 3PA excitation. We obtain a cubic characteristic exponent. (b) Polarization resolved measurement for the 3PA experiment. (c) Time-resolved PL for PL-2PA and the 3PA excitation.

the intrinsic radiative lifetime of the QD. We firmly believe that our results shed new light on the fundamental quantum-mechanical selection rules describing two-level systems and open up routes to implementing new resonant protocols for state preparation and quantum control.

We gratefully acknowledge financial support from the German Federal Ministry of Education and Research via the funding program Photonics Research Germany (contract number 13N14846, the BMBF via the project Q.Link.X (16KIS0874) and QR.X (16KISQ027) and the Deutsche Forschungsgemeinschaft (DFG, German Research Foundation) under Germany's Excellence Strategy – EXC-2111 – 390814868. V. Villafañe gratefully acknowledges the MCQST Distinguished Fellowship program and the Alexander v. Humboldt foundation for financial support in the framework of their fellowship programmes.

* Contributed equally to this work.
† Electronic address: kai.mueller@wsi.tum.de

[1] C. Dory, K. A. Fischer, K. Müller, K. G. Lagoudakis, T. Sarmiento, A. Rundquist, J. L. Zhang, Y. Kelaita, and J. Vučković, Scientific reports **6**, 1 (2016).
[2] F. Sbresny, L. Hanschke, E. Schöll, W. Rauhaus, B. Scaparra, K. Boos, H. Riedl, J. J. Finley, K. Jöns, and K. Müller, *Stimulated generation of indistinguishable single photons from a quantum ladder system* (2021), 2107.03232.
[3] D. Press, T. D. Ladd, B. Zhang, and Y. Yamamoto, Nature **456**, 218 (2008).

[4] P. Cerfontaine, T. Botzem, J. Ritzmann, S. S. Humpohl, A. Ludwig, D. Schuh, D. Bougeard, A. D. Wieck, and H. Bluhm, Nature communications **11**, 1 (2020).

[5] T. Stievater, X. Li, D. G. Steel, D. Gammon, D. Katzer, D. Park, C. Piermarocchi, and L. Sham, Physical Review Letters **87**, 133603 (2001).

[6] A. Zrenner, E. Beham, S. Stufler, F. Findeis, M. Bichler, and G. Abstreiter, Nature **418**, 612 (2002).

[7] A. Ramsay, Semiconductor Science and Technology **25**, 103001 (2010).

[8] J. H. Shirley, Phys. Rev. **138**, B979 (1965), URL https://link.aps.org/doi/10.1103/PhysRev.138.B979.

[9] T. Wang, T. J. Puchtler, T. Zhu, J. C. Jarman, L. P. Nuttall, R. A. Oliver, and R. A. Taylor, Nanoscale **9**, 9421 (2017), URL http://dx.doi.org/10.1039/C7NR03391E.

[10] S. K. Patra and S. Schulz, Nano letters **20**, 234 (2019).

[11] L. Zhang, C.-H. Teng, P.-C. Ku, and H. Deng, Physical Review B **93**, 085301 (2016).

[12] S. Kako, C. Santori, K. Hoshino, S. Götzinger, Y. Yamamoto, and Y. Arakawa, Nature materials **5**, 887 (2006).

[13] S. Sultana and M. S. Alam, in *2015 18th International Conference on Computer and Information Technology (ICCIT)* (IEEE, 2015), pp. 550–553.

[14] L. Y. Lee, Materials Science and Technology **33**, 1570 (2017).

[15] T. Zhu, F. Oehler, B. P. L. Reid, R. M. Emery, R. A. Taylor, M. J. Kappers, and R. A. Oliver, Applied Physics Letters **102**, 251905 (2013), https://doi.org/10.1063/1.4812345, URL https://doi.org/10.1063/1.4812345.

[16] J. T. Griffiths, T. Zhu, F. Oehler, R. M. Emery, W. Y. Fu, B. P. L. Reid, R. A. Taylor, M. J. Kappers, C. J. Humphreys, and R. A. Oliver, APL Materials **2**, 126101 (2014), https://doi.org/10.1063/1.4904068, URL https://doi.org/10.1063/1.4904068.

[17] B. P. L. Reid, T. Zhu, C. C. S. Chan, C. Kocher, F. Oehler, R. Emery, M. J. Kappers, R. A. Oliver, and R. A. Taylor, physica status solidi c **11**, 702 (2014), https://onlinelibrary.wiley.com/doi/pdf/10.1002/pssc.201300666, URL https://onlinelibrary.wiley.com/doi/abs/10.1002/pssc.201300666.

[18] A. Jarjour, T. Parker, R. Taylor, R. Martin, and I. Watson, physica status solidi (c) **2**, 3843 (2005).

[19] D. Collins, A. Jarjour, M. Hadjipanayi, R. Taylor, R. Oliver, M. Kappers, C. Humphreys, and A. Tahraoui, Nanotechnology **20**, 245702 (2009).

[20] C.-K. Sun, S.-W. Chu, S.-P. Tai, S. Keller, U. K. Mishra, and S. P. DenBaars, Applied Physics Letters **77**, 2331 (2000), https://doi.org/10.1063/1.1316776, URL https://doi.org/10.1063/1.1316776.

[21] C.-K. Sun, S.-W. Chu, S.-P. Tai, S. Keller, A. Abare, U. K. Mishra, and S. P. Denbaars, Scanning **23**, 182 (2001), https://onlinelibrary.wiley.com/doi/pdf/10.1002/sca.4950230304, URL https://onlinelibrary.wiley.com/doi/abs/10.1002/sca.4950230304.

[22] M. A. Reshchikov, Journal of Applied Physics **129**, 121101 (2021), https://doi.org/10.1063/5.0041608, URL https://doi.org/10.1063/5.0041608.

[23] M. A. Reshchikov, M. Vorobiov, K. Grabianska, M. Zajac, M. Iwinska, and M. Bockowski, Journal of Applied Physics **129**, 095703 (2021), https://doi.org/10.1063/5.0045019, URL https://doi.org/10.1063/5.0045019.

[24] A. D. Lad, P. P. Kiran, D. More, G. R. Kumar, and S. Mahamuni, Applied Physics Letters **92**, 043126 (2008).

[25] N. S. Makarov, P. C. Lau, C. Olson, K. A. Velizhanin, K. M. Solntsev, K. Kieu, S. Kilina, S. Tretiak, R. A. Norwood, N. Peyghambarian, et al., ACS nano **8**, 12572 (2014).

[26] J. Johansson, P. Nation, and F. Nori, Computer Physics Communications **183**, 1760 (2012), ISSN 0010-4655, URL https://www.sciencedirect.com/science/article/pii/S0010465512000835.

[27] J. Johansson, P. Nation, and F. Nori, Computer Physics Communications **184**, 1234 (2013), ISSN 0010-4655, URL https://www.sciencedirect.com/science/article/pii/S0010465512003955.

[28] A. Thränhardt, C. Ell, G. Khitrova, and H. M. Gibbs, Phys. Rev. B **65**, 035327 (2002), URL https://link.aps.org/doi/10.1103/PhysRevB.65.035327.

[29] I. A. Ostapenko, G. Hönig, C. Kindel, S. Rodt, A. Strittmatter, A. Hoffmann, and D. Bimberg, Applied Physics Letters **97**, 063103 (2010), https://doi.org/10.1063/1.3477952, URL https://doi.org/10.1063/1.3477952.